MICROSCOPY

Microscopy, 2020, 350–359
doi: 10.1093/jmicro/dfaa028
Advance Access Publication Date: 23 May 2020

Article

Improved unroofing protocols for cryo-electron microscopy, atomic force microscopy and freeze-etching electron microscopy and the associated mechanisms

Nobuhiro Morone[1], Eiji Usukura[2], Akihiro Narita[3], and Jiro Usukura[2,*]

[1]Medical Research Council Toxicology Unit, University of Cambridge, Lancaster Road, Leicester LE1 9HN, UK, [2] Institute of Materials and Systems for Sustainability, Nagoya University, Chikusa-ku, Nagoya 464-8601, Japan, and [3] Structural Biology Research Centre, Graduate School of Science, Nagoya University, Chikusa-ku,Nagoya,464-8601, Japan

*To whom correspondence should be addressed. E-mail: usukura@imass.nagoya-u.ac.jp

Received 10 March 2020; Revised 5 May 2020; Accepted 18 May 2020

Abstract

Unroofing, which is the mechanical shearing of a cell to expose the cytoplasmic surface of the cell membrane, is a unique preparation method that allows membrane cytoskeletons to be observed by cryo-electron microscopy, atomic force microscopy, freeze-etching electron microscopy and other methods. Ultrasound and adhesion have been known to mechanically unroof cells. In this study, unroofing using these two means was denoted sonication unroofing and adhesion unroofing, respectively. We clarified the mechanisms by which cell membranes are removed in these unroofing procedures and established efficient protocols for each based on the mechanisms. In sonication unroofing, fine bubbles generated by sonication adhered electrostatically to apical cell surfaces and then removed the apical (dorsal) cell membrane with the assistance of buoyancy and water flow. The cytoplasmic surface of the ventral cell membrane remaining on the grids became observable by this method. In adhesion unroofing, grids charged positively by coating with Alcian blue were pressed onto the cells, thereby tightly adsorbing the dorsal cell membrane. Subsequently, a part of the cell membrane strongly adhered to the grids was peeled from the cells and transferred onto the grids when the grids were lifted. This method thus allowed the visualization of the cytoplasmic surface of the dorsal cell membrane. This paper describes robust, improved protocols for the two unroofing methods in detail. In addition, micro-unroofing (perforation) likely due to nanobubbles is introduced as a new method to make cells transparent to electron beams.

Key words: unroofing, cell membrane, cytoskeleton, actin filaments, cryo-electron microscopy, atomic force microscopy

Introduction

Unroofing is not a new preparation method in a strict sense, as it has been used repeatedly in the history of imaging the cytoplasmic surface (i.e. inner surface) of the cell membrane. Structural information regarding the membrane-associated cytoskeleton (i.e. membrane cytoskeleton) and organelles is vital for understanding essential functions related to infection, endocytosis, signal transduction and motility. Therefore, it is essential to establish a preparation method for observing these structures under various microscopes. Orthodox unroofing involves the mechanical shearing of cells, whereupon the soluble cytoplasm and several organelles flow out concomitantly upon the disruption of the cell membrane,

rendering the inner surface of the cell membrane exposed and visible. Unroofing is a unique preparation method that must be performed to observe the membrane cytoskeleton and associated structures in cryo-electron microscopy (cryo-EM), atomic force microscopy (AFM) and freeze-etching replica electron microscopy (freeze-etch EM). Notably, unroofing enabled the display of intracellular structures via AFM for the first time [1,2] because the procedure allowed AFM cantilever tips to be placed directly on intracellular structures. Generally, unroofing is easier if the cells are firmly attached to the substrate. Therefore, the unroofing procedure has closely involved the use of poly-L-lysine (PLL) to adhere cells onto the substrate [3–5] (see also the review in [6]). In early days, after cells were tethered onto the substrate, the apical cell membrane and cytoplasm were swept away with a squirt of Ringer's solution or buffer expelled from a Pasteur pipette or the needle of a syringe [4,5,7–9]. A ventral cell membrane adhered firmly on the substrate with PLL is left intact, even when the apical portion of a cell is ablated to a considerable extent. However, this type of unroofing required technical skill and produced a low yield. The urgent need to observe the intracellular cytoskeleton under electron microscopy inspired the use of detergents such as Triton X or saponin to elute the cytoplasm, resulting in a type of chemical unroofing [10–17]. This detergent-induced unroofing has been used frequently because the chemical dissolution of the cell membrane is much easier to achieve than mechanical unroofing. It is believed that the cytoskeleton is detergent insoluble, and the spatial arrangement of the cytoskeleton in cells is therefore considered to remain intact after treatment with detergents. However, the membrane and membrane-associated structures (i.e. caveolae and clathrin-coated vesicles), membrane cytoskeleton and endoplasmic reticulum (ER) network are completely removed by the dissolution of the membrane lipids. The interaction between the cytoskeleton and the inner surface of the membrane is lost as well. Under these circumstances, Heuser [18,19] first introduced sonication as an effective tool for unroofing in freeze-etch EM. Compared with a squirt of Ringer's solution, sonication produced good results in terms of reproducibility and image quality. Unroofing via sonication is used in freeze-etch EM [18–24], and in platinum replica electron microscopy, it is combined with critical point drying [25] owing to the high quality of the resultant image at high magnification. However, sonication unroofing still requires some experience to obtain successful results. The commercially available horn-type ultrasonic generator was originally designed as a homogenizer with high-output power (greater than 50 W) and precisely regulated the power in only the high-power regime (~10–50 W). Whole cells disappeared immediately upon exposure to such high-power sonication. In contrast, the optimal output power for unroofing was 0.5–0.8 W in our experiments. Therefore, the specimen must be held motionless by hand at an appropriate distance from the tip of the horn, even under the lowest power of the device (~5–10 W, varying among product makers). To overcome this difficulty, the ultrasonic generator was customized to also regulate the power from 0–1 W to optimize the sonication unroofing procedure and increase its efficiency. An alternative mechanical unroofing method uses adhesive glue (named here adhesion unroofing for convenience) and is designed to allow the inner surface of the dorsal cell membrane to be observed. In brief, this method peels away the apical membrane using an adhesive mesh grid or coverslip coated with Alcian blue. Adhesion unroofing is a mild unroofing compared with sonication unroofing, where fine bubbles stir the buffer during unroofing. Therefore, adhesion unroofing is suitable for observing delicate intracellular structures despite its low yield. Different procedures are used for adhesion unroofing depending on the purpose of the study. Practically, this method has been used for several decades with some modifications [26–34] because no special equipment is required. Adhesion unroofing is also known by various other names, including the rip-off method, the squashing method and the sandwich method. The above two kinds of unroofing methods using sonication or adhesive glue were improved in this study for application to cryo-EM and AFM. In this paper, the optimized protocols to increase the efficiency of the two unroofing methods are described in detail, and the mechanisms involved are explained.

Methods

Preparation of reagents

The following solutions used in sonication unroofing and adhesion unroofing were prepared before each experiment:

(i) HEPES-based mammalian Ringer's solution: 155 mM NaCl, 3 mM KCl, 2 mM $CaCl_2$, 1 mM $MgCl_2$, 3 mM NaH_2PO_4, 10 mM glucose and 5 mM HEPES (pH 7.4) [6]. HEPES: 4-2(2-hydroxyethyl)-1-piperazineethanesulfonic acid.

(ii) Ca-free HEPES-based mammalian Ringer's solution: As the Ringer's solution above but without $CaCl_2$.

(iii) PLL solution: Poly-L-lysine (MW 30,000–50,000: Sigma-Aldrich, St. Louis, MO, USA) was dissolved in in Ca^{2+}-free Ringer's solution at a concentration of 0.5 mg ml^{-1}. This reagent was used exclusively for sonication unroofing and was filtered through Millipore filters (Millex Syringe Filter SLGSV255F: Merck KGaA, Darmstadt, Germany) prior to use.

(iv) Isotonic KHMgE buffer: 30 mM HEPES, 70 mM KCl, 3 mM $MgCl_2$ and 1 mM EGTA (slightly modified from the original recipe [6]), which was adjusted to pH 7.4 with KOH. EGTA: ethylene glycol tetra-acetic acid (Dojindo Laboratories, Kumamoto, Japan).

(v) Hypotonic KHMgE buffer: One part isotonic KHMgE buffer was mixed with two parts distilled water (DW).

(vi) Unroofing buffer: Isotonic KHMgE buffer with 0.1 mM AEBSF as a protease inhibitor. Protease inhibitor was added just prior to use.
AEBSF: 4-(2-Aminoethyl) benzene sulfonyl fluoride hydrochloride (Pefabloc SC, Roche, Basel, Switzerland). Other protease inhibitors or inhibitor cocktails may be used if they are soluble in water.

(vii) Alcian blue solution: Alcian blue (MP Biomedical LLC, OH, USA) powder was dissolved in DW water to 1% (volume weight percent) and was used to produce adhesive mesh grids or coverslips for adhesion unroofing.

Equipment for sonication unroofing

A horn-type ultrasonic generator was customized to be regulated within the low-power region (0–10 W, 27 kHz) (UR-21PS Tomy-seiko Co., Tokyo, Japan).

A dissecting microscope (SZ-61, Olympus Corporation, Tokyo, Japan) was set up with an assistance device (position controller) that holds the horn-type probe in a hands-free manner and is able to change the vertical position, the front-back position and the tilt as shown in Fig. 1. More recently, another assistance device similar to the above position controller (Hitachi High-Technologies Corporation, Tokyo, Japan) was combined with an inverted phase-contrast light microscope (CKX-53, Olympus Corporation, Tokyo) to determine the optimal degree of unroofing by monitoring the unroofing process with a video camera (Fig. 2).

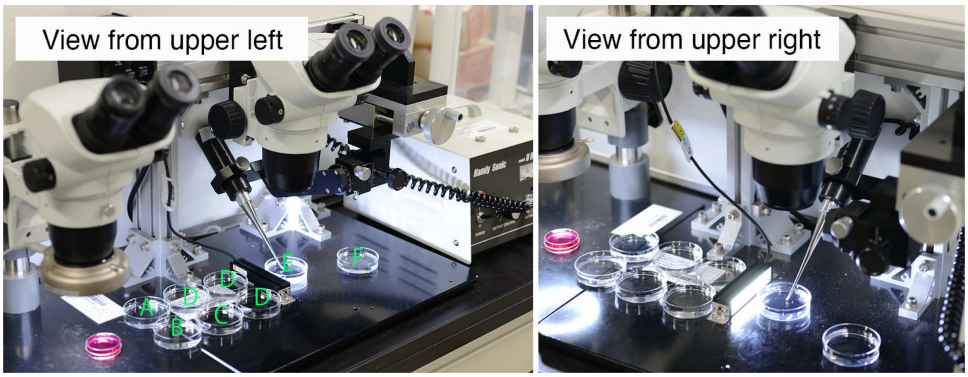

Fig. 1. Unroofing setup consisting of a dissecting microscope, customized ultrasonic generator and an assistance device (position controller: See text for explanation). Photographs of the setup from the upper right (right image) and upper left (left image) showing the solutions A: HEPES-based Ringer's solution. B: Ca-free HEPES-based Ringer's solution. C: Poly-L-lysine (PLL) dissolved in Ca-free HEPES-based Ringer's solution (0.5 mg ml^{-1}). D: Hypotonic or isotonic KHMgE buffer. E: Unroofing buffer. F: Fresh unroofing buffer for washing unroofed cells.

Fig. 2. New unroofing setup consisting of an inverted phase-contrast microscope equipped with a video camera, customized ultrasonic generator and an assistance device holding the horn-type probe in a hands-free manner.

Equipment for adhesion unroofing

Using a dissection microscope during adhesion unroofing can be convenient for handling mesh grids and small coverslips, but it is not always necessary for individuals with good vision.

Procedure of sonication unroofing

(i) Cells were cultured on C-flat gold mesh grids (#200) or molybdenum mesh grids (#200) covered with carbon-coated Formvar (polyvinyl formal) for cryo-EM, small coverslips (2.5 mm × 2.5 mm, Matsunami micro cover glass, thickness no.1 Matsunami Glass IND. LTD, Osaka, Japan) for freeze-etch EM or an appropriate substrate for AFM (Fig. 3, Step 1). The mesh grids and substrate were hydrophilized with plasma ion discharge followed by disinfection with 70% alcohol prior to initiating the cell culture (Fig. 3).

(ii) Cells were sequentially washed with Ca-plus and then Ca-free Ringer's solution for a few seconds each to remove the culture medium (Fig. 3, Step 2). Ca-free Ringer's solution was used to prevent the aggregation of PLL due to Ca ions when cells were immersed in PLL in the next step.

(iii) Cells were soaked in PLL solution for ∼5–8 s (Fig. 3, Step 3). In this step, the cells became more firmly attached to the substrate, and the cell surfaces were covered with positively charged PLL.

(iv) The cells were washed three times (for 2–3 s each) in hypotonic KHMgE buffer. This step was performed to remove the unbound PLL, but it also swelled the cells slightly so that they burst easily during sonication. However, when hypotonic buffer use is avoided for the protection of delicate structures or the aim of research, isotonic buffer may be used to wash away unbound PLL instead of hypotonic buffer (Fig. 3, Step 4).

(v) Immediately after washing away the unbound PLL, the cells were exposed to fine bubbles generated by weak sonication (0.5 W, 27 kHz) in the unroofing buffer for ∼10 s (Fig. 3, Step 5). As shown in Fig. 4 and Supplementary Video 1 online, the sample was placed 2–3 mm away from the tip of the horn.

(vi) The unroofed cells were washed again for 2–3 s with slight shaking in fresh unroofing buffer to remove debris from the specimen surface and were processed promptly according to the observation method (Fig. 3, Step 6).

(vii) (a) For cryo-EM, unroofed cells on mesh grids were quickly frozen in liquid ethane using a Leica EM GP plunger. The frozen samples were mounted on a cryo-transfer holder and observed directly under a cryo-electron microscope.

(vii) (b) For freeze-etch EM or AFM, unroofed cells were typically fixed with 2% glutaraldehyde in KHMgE buffer for 20 min. Samples were washed twice with phosphate-buffered saline (PBS) after fixation. When immunological labelling is necessary to identify the constituent proteins of certain structures, samples should be incubated with a primary antibody after this step. Finally, unroofed fixed cells were washed well in DW just prior to rapid freezing. For AFM observation, unroofed and fixed cells were examined directly by AFM in PBS or DW.

Procedure of adhesion unroofing

The adhesive mesh grids or coverslips used for picking up the dorsal cell membrane must be prepared prior to the experiments

For cryo-EM, C-flat gold mesh grids (#200) or molybdenum mesh grids (#200) covered with carbon-coated Formvar were used to collect the membrane. The mesh grids must be flat for efficient peel-off. If there were even small dents in a mesh grid, it was not usable. For freeze-etch EM, small coverslips (2.5 mm × 2.5 mm) were commonly used to collect the cell membrane. In the case of AFM, the specimen stage and substrate used for measurement generally varied

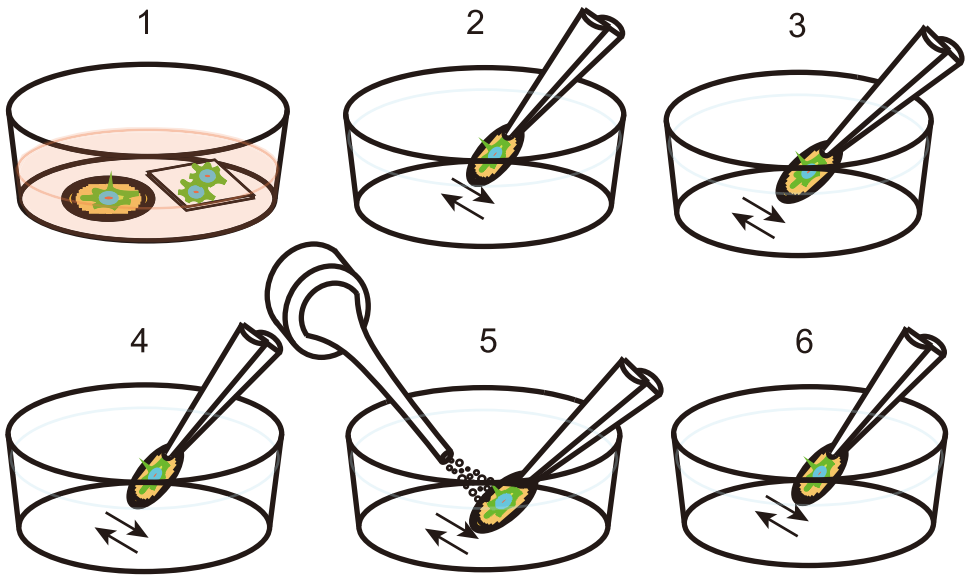

Fig. 3. Schematic illustration of the procedure for sonication unroofing. The numbers in the figure correspond to the step numbers in the procedure in the text. 1. Cell culture. 2. Removing the culture medium by washing with Ringer's solution and Ca-free Ringer's sequentially with gentle shaking. 3. Soaking in PLL solution. 4. Washing the samples three times with hypotonic buffer or isotonic buffer for removing unbound PLL with gentle shaking. 5. Unroofing cells with fine bubbles generated by sonication in unroofing buffer. 6. Washing unroofed cells in fresh unroofing buffer to remove debris with gentle shaking.

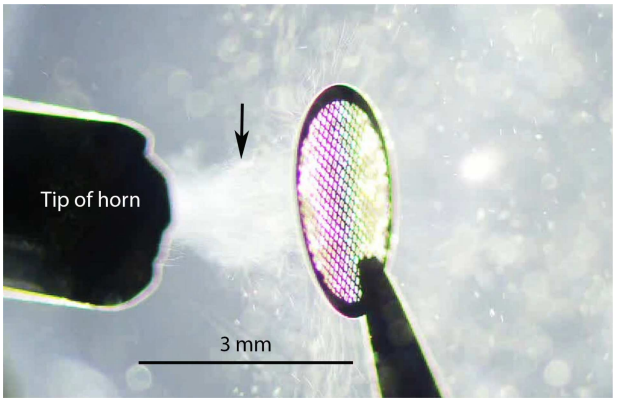

Fig. 4. Phase-contrast optical micrograph showing the positional relationship between the sample and the tip of the horn for ultrasonic generation in sonication unroofing. The arrow indicates a stream of fine bubbles.

among manufacturers. Each step of the following procedure must be modified slightly according to the substrate for AFM (Fig. 5).

Grids or coverslips were hydrophilized with a plasma ion discharger and then soaked in 1% Alcian blue solution in DW for 2 min. After being washed twice in DW (10 s each), the mesh grids and coverslips were kept clean and dry until use. Adhesive mesh grids or coverslips were prepared less than 3 h before the experiments because the adhesive properties decreased with time. PLL is very sticky as a glue and may also be used instead of Alcian blue. However, we preferred to use Alcian blue because PLL is a much larger molecule that can be observed by EM, and unbound PLL sometimes attaches to a fresh unroofed surface and becomes a source of contamination. Therefore, we employed Alcian blue instead of PLL despite its weaker adhesive strength.

(i) Cells were cultured on a small square coverslip (2.5 mm × 2.5 mm) (Fig. 5, Step 1). These coverslips must be hydrophilized with plasma ion discharge followed by disinfection with 70% alcohol prior to initiating cell culture.

(ii) Cells cultured on the coverslip were washed sequentially with Ca-plus and then Ca-free Ringer's solution for a few seconds each to remove the culture medium (Fig. 5, Step 2).

(iii) Cells were further washed in unroofing buffer for a few seconds (Fig. 5, Step 2).

(iv) The washed cells on coverslips were placed in new Petri dishes, as shown in Fig. 5, Step 3.

(v) For cryo-EM, Alcian blue-treated C-flat gold mesh grids or molybdenum mesh grids covered with carbon-coated Formvar were placed on the cells cultured on coverslips (Fig. 5, Step 4). For freeze-etch EM or AFM, instead of mesh grids, Alcian blue-treated coverslips (2.5 mm × 2.5 mm) were placed on the cells (Fig. 5, Step 4′).

(vi) Any excess amount of unroofing buffer was absorbed with filter paper so that the grids or coverslips contacted the cells firmly (Fig. 5 Step 5 or Step 5′).

(vii) When necessary, a small piece of glass was placed on the grid as a weight. In this way, the cells were squashed gently, and the unroofing efficiency was increased. A glass slide was cut into small pieces (5 mm × 5 mm square) with a cutter, and one of these pieces was used as a weight in this study (Fig. 5, Step 6).

(viii) (a) For cryo-EM, after squashing the cells with the adhesive grid for 1 min, the grid was lifted from the cells by pouring 500 µL of unroofing buffer over the unroofing setup (Fig. 5, Step 7). In this process, the dorsal cell membrane with the membrane cytoskeleton was torn off onto the mesh grids (Fig. 5, Step 8). Dorsal membrane fractions attached to the grid were washed to remove debris in fresh buffer for a few seconds and frozen quickly in liquid ethane using a Leica EM GP plunger.

(viii) (b) For AFM or freeze-etch EM, after absorbing the excess amount of unroofing buffer with filter paper (Fig. 5, Step 5′)

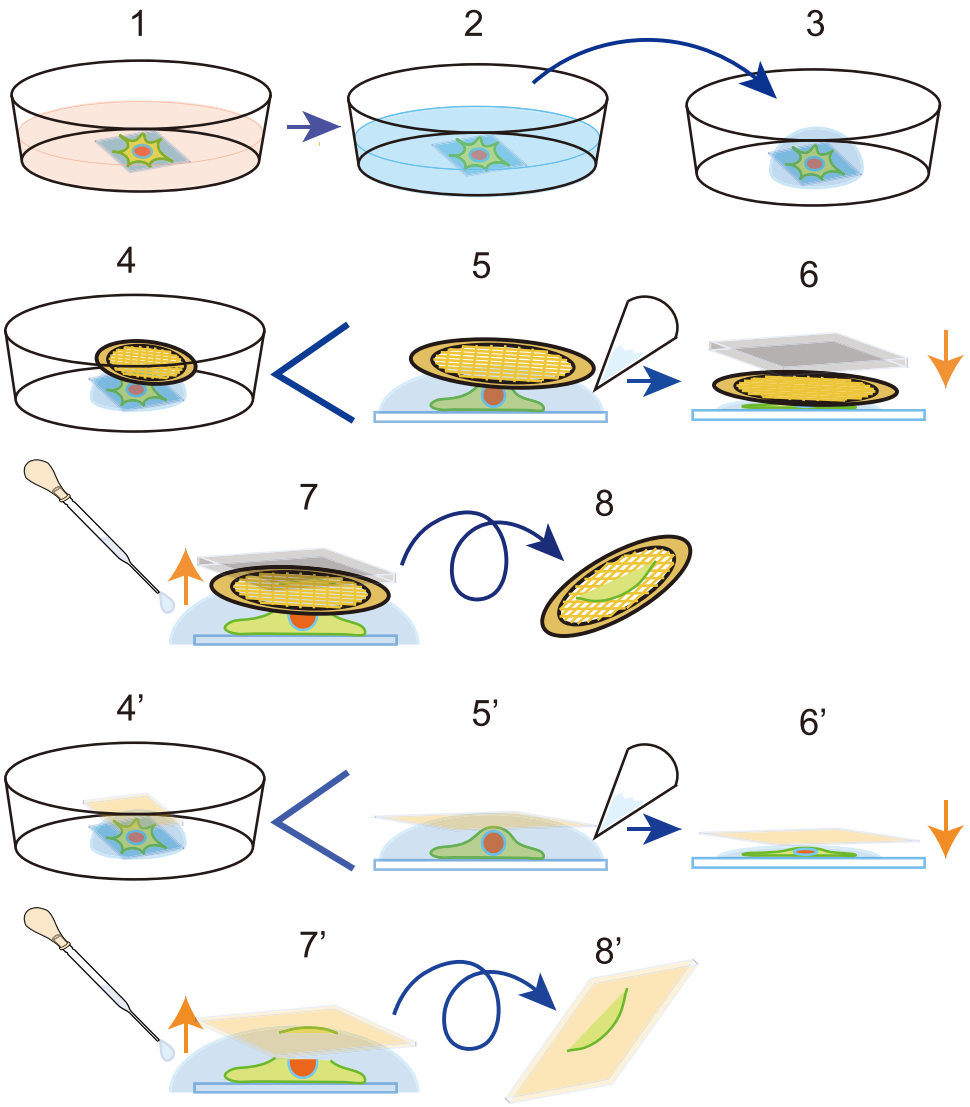

Fig. 5. Schematic illustration of the adhesion unroofing procedure. The number labels of each step in the figure correspond to experimental steps described in the text. 1. Cell culture on the coverslips (2.5 mm × 2.5 mm). 2. Removing the culture medium by washing with Ringer's solution and subsequent unroofing buffer. 3. Placing the samples in new dish. 4. Placing a sticky grid on the cells. 5. Absorbing excess buffer with a filter paper. 6. Placing a small glass slide (5 mm × 5 mm) as a weight. 7. Lifting the grid from cells by pouring 300 ml of unroofing buffer. 8. Transferring the dorsal cell membrane onto the grid. Steps 1–8 are for cryo-EM. Steps 4′–8′ are for AFM or freeze-etch EM.

and maintaining contact for 1 min (Fig. 5, Step 6′), the upper coverslip was lifted by pouring fixative (2% glutaraldehyde in KHMgE buffer) over the unroofing setup (Fig. 5, Step 7′). The dorsal cell membranes were peeled off onto the upper coverslip (Fig. 5, Step 8′). The specimens on the coverslip were further fixed for 10 min in the same fixative and then washed in KHMgE buffer. In AFM, specimens were observed directly in buffer. In freeze-etch EM, the specimens were further washed well with DW and then quickly frozen using a high-pressure freezing apparatus or a device that quickly freezes a sample by contact with metal.

Microscopes used in this study

For the observation of frozen unroofed cells (cryo-EM), an FEI Tecnai G2 Polara and a cryo-specific Hitachi SU9000 were used. The AFM we used was an Olympus BIXAM. Freeze-etching replicas of unroofed cells were observed under a Hitachi H-7600 conventional transmission electron microscope.

This study addresses improved unroofing mechanisms and protocols for application to cryo-EM, AFM and freeze-etch EM in terms of sample preparation methods but does not describe the observation procedures of cryo-EM, AFM and freeze-etch EM. People who are interested in them should refer to papers published previously [1,2,10,31,34,35].

Results

Images of unroofed cells obtained by various microscopy techniques

As detailed in the methods section, the protocols developed in this study significantly increased the success rate of unroofing. The elu-

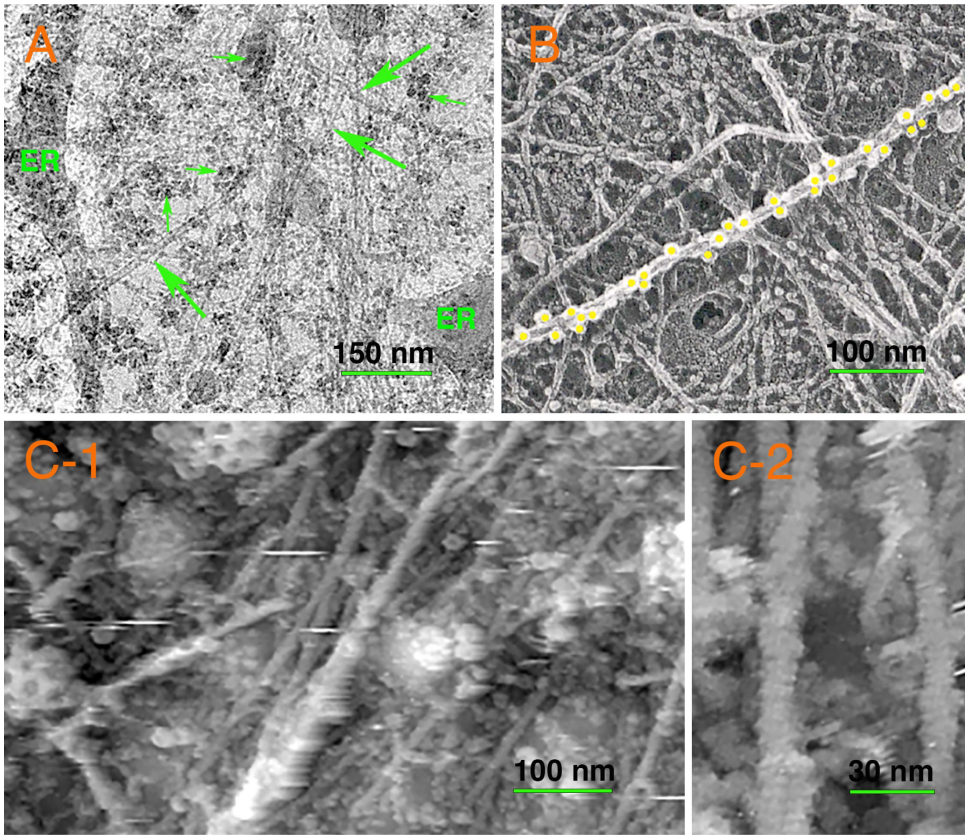

Fig. 6. Gallery of micrographs of unroofed cells obtained by various microscopy techniques. (a) Cryo-electron micrograph of native unroofed cells (NRK cells). Large numbers of cytoskeletal actin filaments, microtubules (arrows), endoplasmic reticulum (ER) parts and ribosomes (small arrows) overlap with each other because the thickness of the sample is much greater (~300 nm) than a conventional electron microscopy thin section. However, the image appears clear under high contrast because the cytoplasm is washed away by unroofing. (b) Immuno-freeze-etch EM micrograph showing the membrane cytoskeleton on the inner surface of a cell membrane exposed by sonication unroofing. Microtubules are labelled with an anti-beta tubulin antibody and then subsequently labelled with a gold conjugated-secondary antibody (coloured in yellow). (c-1) Atomic force micrograph showing the cytoskeleton on the inner surface of ventral cell membrane. (c-2) High-magnification atomic force micrograph showing actin filaments. The short periodicity (5.5 nm) of the actin filaments is displayed clearly. Thus, the cantilever is able to directly scan the cell after unroofing.

cidation of the unroofing mechanism, described below, also allowed the optimization of the protocol. In addition, the development of an assistance device that controls the position of the horn tip greatly improved the yield. These advances enabled unroofing to be used as the preparation method for various microscopies. Such unroofing methods made it possible to observe the three-dimensional structures of the cytoskeleton and organelles attached to the inner surface (i.e. cytoplasmic side) of the cell membrane using various types of microscopies (Fig. 6). In particular, it was impossible to observe intracellular structures at high resolution with AFM without removing the cell membrane. Another feature of unroofing is that the degree of unroofing varies from cell to cell. For example, in some cells, the cytoplasm and cytoskeleton were completely removed, leaving only the clathrin-coated vesicles and caveola on the inner surface of the membrane (Fig. 6). In other cells, many cytoskeleton components remained on the inner surface of the membrane. Therefore, various structures of the inner surface of cell membranes (membrane undercoat) could be observed in even one unroofing experiment.

Mechanism of sonication unroofing

It is essential to understand the mechanism of unroofing to apply this method properly for various microscopies. Therefore, real-time visualization of the unroofing process was obtained under a phase-contrast microscope to clarify why and how the cell membrane is removed during sonication. When a horn-type ultrasonic generator was operated in a buffer solution, a flow of microbubbles and nanobubbles was emitted from the tip of the horn. Such cavitation occurred even under low-power sonication (27 kHz, 0.5 W). As shown in Supplementary Video 2, it became evident that the microbubbles induced by sonication played the leading role in unroofing. First, the microbubbles adhered to the cell surface and sheared the cells with microbubble motion (Fig. 7, see Supplementary Video 2 online). An assistance device was also made to easily and accurately direct fine bubbles onto a sample and to facilitate the positioning of a probe tip of an ultrasonic generator while viewing the process under a dissection microscope. It is further discussed below how the fine bubbles adhere to cell surfaces and shear the membrane.

Mechanism of adhesion unroofing

The mechanism of adhesion unroofing using Alcian blue-coated grids or coverslips is easy to understand. Alcian blue has a positive charge, as seen in its molecular structure, allowing Alcian blue-coated grids or coverslips to become electrostatically glued to the negatively

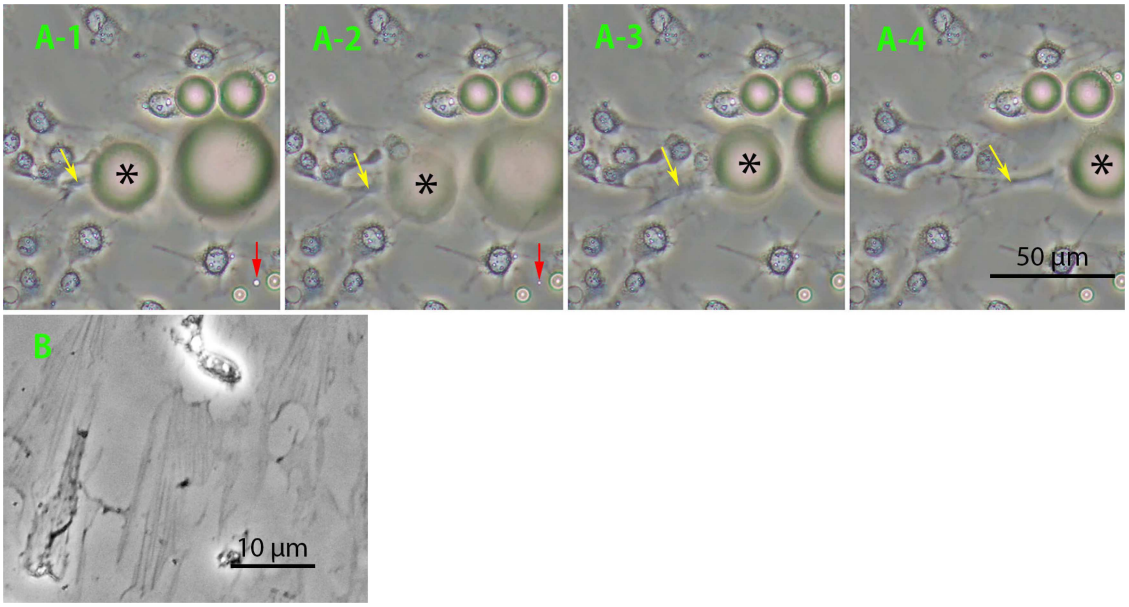

Fig. 7. (a-1–a-4) Continuous scenes from a video recording of sonication unroofing. Microbubbles (asterisks) adhere to a portion of the cell first and then shear it by pulling (yellow arrows). Red arrows indicate nanobubbles during rupture. (b) High-magnification phase-contrast micrograph of unroofed cells showing the membrane cytoskeleton attached to the ventral cell membrane. At low magnification, nothing appears to remain on the substrate after sonication, but increasing the magnification allows the observation of the ventral membrane and the cytoskeleton attached to it.

charged cell surface. The electrostatic adhesion force of Alcian blue is weakened in water, and thus, the yield of dorsal cell membranes peeled off onto the grids was low. However, adhesion unroofing possesses the advantage of making the inner surface of the dorsal cell membrane visible, making it superior for the preservation of delicate structures. This is in contrast to the sonication method, which disrupts the membrane with fine bubbles. Interestingly, mitotic cells appeared to adhere preferentially to the grid or an apical coverslip (Fig. 8). This is because cells in mitosis tend to be rounded, which weakened their binding to the substrate. Frequently, many mitotic cells moved onto the grid together, but in many cases, parts of the ventral cell membrane were left on the substrate. That is, the cells that moved onto the grid were partially unroofed, and as shown in Fig. 8, the chromosomes were sometimes exposed, allowing direct observation with SEM or AFM. In the adhesion method, the adhesive grid was pressed onto the apical cell surface so that the mitotic cells were easily moved onto the grid. The decrease in the force binding the substrate resulted in the loss of the cells and made it difficult to observe mitotic cells via the sonication method. At any rate, adhesion unroofing is a useful method despite its low yield because no special equipment is required for it.

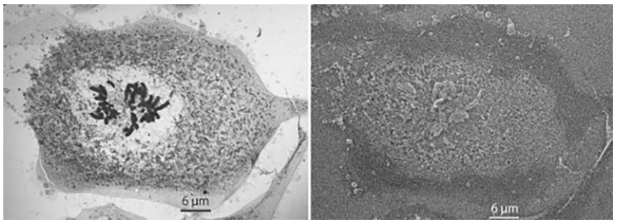

Fig. 8. Simultaneous imaging through cryo-STEM (left) and cryo-SEM (right) of a mitotic anaphase cell unroofed via the adhesion method. As seen from the SEM image (right), part of the ventral cell membrane is peeled off, and the chromosomes are exposed. In the cryo-STEM image (left), chromosomes and organelles are clearly observed although the thickness of cell is much greater than several hundred nanometres.

Discussion

Hypothesized detailed mechanism of sonication unroofing

Generally, the outer surface of the cell membrane is slightly negatively charged as a whole. Therefore, PLL, which exhibits many positive charges, binds it easily. After modification with many PLL molecules, the outer surface of the cell membrane is positively charged. Furthermore, microbubble surfaces are considered negatively charged, as shown in a previous study [36], which is why microbubbles adhere to the cell surface. Microbubbles electrostatically bound to the surface of the cell membrane gradually ruptured the cell membrane through buoyancy and fluid flow forces. The PLL not only connects cells to the substrate but also positively charges the cell surface. Thus, PLL processing is an important step in the sonication unroofing procedure. Such an unroofing mechanism, derived from video analysis, is summarized according to the scheme in Fig. 9.

Discovery and usefulness of another micro-unroofing (perforation) that is hidden by large-scale sonication unroofing

Sonication unroofing is a method for shearing cells by exposing them to a stream of micro- and nanobubbles generated by sonication. Video analysis of the unroofing process reveals that the microbubbles play a key role in unroofing (Fig. 6 and see Supplementary Video 2 online). In some cases, microbubbles will shear off the entire cell membrane while forming a cluster (see Supplementary Video 2 online). It is difficult to clearly visualize nanobubbles as bubbles under an optical microscope, but in Supplementary Video 2, they can

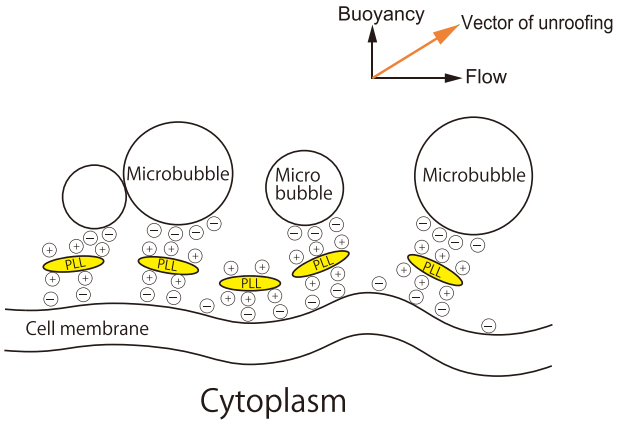

Fig. 9. Schematic illustration of how microbubbles adhere to the cell membrane in sonication unroofing. The positively charged PLL adheres to the cell membrane and neutralizes the negative charge of the cell surface, while the excess positive charge of the PLL covers the cells. Because microbubbles are partially negatively charged, they become attached to the cell membrane via the PLL. The membrane is torn off by the combined force of the buoyancy of the bubbles and the flowing force of the solution. +: positive charge; −: negative charge. Upper right inset shows a vectoral sum diagram. The arrow vector lengths are arbitrary.

be identified as small bright blinking spots. Such observations suggest that nanobubbles have a short lifetime and rupture as soon as they come into contact with the sample. Therefore, their role in unroofing remains to be determined. However, careful analysis of the video shows that the local cell contrast appears to be altered after rupture of the nanobubbles (Fig. 10). Such contrast alteration suggests that cell membrane perforation occurs via the shock wave created when the nanobubbles burst, and the cytoplasm flowing out from there may change the contrast. Although nano- and microbubbles are thought to be generated simultaneously by sonication, there is a difference in the timing with which they impact and react with cells. Specifically, the effect of the nanobubbles on the cells was clearly detectable during only the first few seconds after exposure to the bubble stream generated by weak sonication because perforation by the nanobubbles was hidden by full-scale shearing owing to the microbubble impact several seconds later. In fact, some cells exposed to the flow of bubbles for a few seconds were still undamaged, so they appeared to be several microns thick, but intracellular mitochondria and the ER were clearly observed (Fig. 11). It is as if the cells were transparent to the electron beam. Perhaps the nanobubbles generate several perforations in the membrane from which soluble cytoplasm flowed out. Nevertheless, it is worth noting that there were many parts of the ER just beneath the cell membrane, which were linked to each other and surrounded the whole cell (Fig. 11). It is possible that soluble components of these cells flowed out through small holes in the cell membrane (i.e. perforation) that were probably caused by nanobubbles. To detect only the perforation effect of the nanobubbles, sonication should be completed within a few seconds (i.e. brief sonication). Such brief sonication unroofing may be useful for observing fine intracellular structures, including organelles, in cryo-EM in the future.

Common issues experienced in unroofing experiments

During sonication unroofing, the most common difficulty is excessive cell destruction and loss owing to high sonication intensity. One approach to prevent this is to increase the distance between the probe tip and the sample. However, the distance from the probe tip to the sample and the degree of unroofing are neither proportional nor inversely proportional. If the sample is 1 cm or more away from the tip of the probe, it cannot be unroofed, even if the output is increased to 2 W or more. Therefore, the best way to customize the ultrasonic generator is to regulate the output power from 0.5 to 1 W.

Fig. 10. Magnified images of a portion of a video in chronological order (1–3). If the nanobubbles are several hundred nanometers in diameter, they appear as bright spots with halation (arrows), even under a phase-contrast optical microscope. Upon the rupture of the nanobubbles, the area becomes slightly brighter (dashed circle). This is thought to be owing to holes in the membrane and the cytoplasm flowing out.

When cells were cultured on molybdenum or gold grids covered with carbon-coated Formval film and used as a sample, the carbon-coated Formval film was often completely fragmented, even at a low sonication output. Initially, the Formval film is a strong support membrane, but it tends to deteriorate over time. The support membrane should thus be produced using a Formval solution prepared within 4 months, if possible.

Another difficulty that may be encountered is contamination by PLL in sonication unroofing. Following buffer stirring via sonication, the PLL-containing debris that was released from the cells frequently re-adheres to newly unroofed cell surfaces. The medium-chain PLL used in this experiment had a molecular weight of 30 000–50 000 and was observed as contamination under an electron microscope. Therefore, immediately after unroofing, it is important to perform several seconds of washing by shaking the sample in fresh unroofing buffer. However, as mentioned above, PLL not only tethers the cells to the substrate but also adds positive charges to the cell surface by covering the entire cell. This makes it easier to attach negatively charged microbubbles to the cell surface. For this reason, PLL processing is an essential step for sonication unroofing, and omitting this step will reduce the efficiency of unroofing. In contrast, Alcian blue has a low molecular weight and therefore does not appear under an electron microscope at magnifications of 100 000 times or lower or cause image contamination. Although the cytotoxicity of the cupric compound Alcian blue is not clear, soaking the cell directly in Alcian blue solution instead of PLL solution is not recommended. Moreover, since the positive charge per molecule is small, Alcian blue is not a substitute for PLL in sonication unroofing. In adhesion unroofing, the grid coated with Alcian blue is thoroughly washed, dried and used as an adhesive for picking up the cell membrane, which is less toxic to cells. The adhesive strength of the grid coated with Alcian blue in this way seems to be weak compared with that of the PLL-coated grid. However, as mentioned above, Alcian blue itself does not contaminated images. In addition, other contaminants seem to poorly adhere due to their weak adsorption force, so we prefer to use Alcian blue in adhesion unroofing.

Because unroofing is the mechanical removal of the cell membrane as described above, the unroofing buffer used is also very important to maintain the intracellular structure in the native state. The ion composition of the unroofing buffer must be equivalent

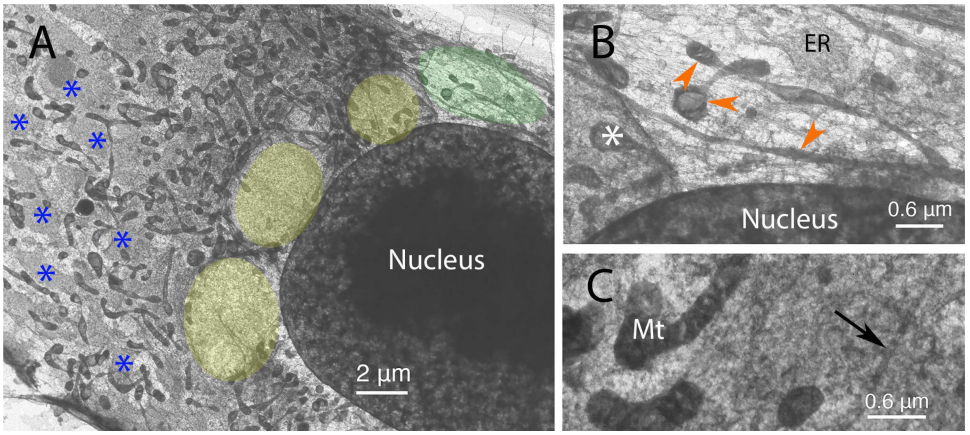

Fig. 11. Cryo-EM images of a cell perforated by brief sonication. (a) Low-magnification image of a perforated cell. The areas without a cell membrane are coloured yellow or green. The regions in yellow are considered holes instantaneously opened by shock waves generated by the bursting of nanobubbles. The green region is considered partially unroofed by ordinary shearing. Blue asterisks (*) indicate parts of the ER just beneath the cell membrane, which were linked to each other and surround the whole cell. (b) High magnification of the green region in (a). The ER and many actin filaments are clearly observed because many cytoplasmic soluble components are eluted. Arrow heads show deformed mitochondria because of changes in the cytoplasmic environment due to unroofing. The asterisk indicates an area between green and yellow regions that is still covered with a cell membrane. (c) Enlarged image of a portion of (a) covered with cell membrane. Because the cytoplasm remains to some degree, the mitochondria (Mt) remain intact. Microtubules (arrow) and many filaments are retained, though they do not clearly correspond with the partially unroofed area (green area in a).

to that of the cytoplasm to maintain the spatial arrangement of the cytoskeleton. For this purpose, the HEPES buffer used herein contained K and Mg instead of Na and Ca. In addition, proteinase inhibitors should also be added to the unroofing buffer.

Concluding remarks

Unroofing is a very useful preparation method for structural analysis of the inner surface of a cell membrane and the cytoskeleton in cryo-EM, AFM and freeze-etch EM. The improved protocol and the developed equipment setup presented in this study increased the yield of unroofing. Real-time video recordings of the unroofing revealed the mechanism by which the fine bubbles generated by sonication in the buffer solution attached to the cell surface and sheared off the membrane via buoyancy and a flowing force. Elucidation of the unroofing mechanism will accelerate the application of this method to various microscopies. In addition, a detailed analysis of the mechanism and careful observation revealed another micro-unroofing (perforation of the cell membrane by nanobubbles) hidden by the large-scale unroofing.

Supplementary data

Supplementary data are available at *Microscopy* online.

Author contributions

J.U. developed devices for sonication unroofing. J.U. and E.U. clarified the mechanisms of unroofing and improved the protocols of sonication unroofing and adhesion unroofing for AFM and cryo-EM. N. M. and J.U. applied unroofing to freeze-etch EM. A.N. was in charge of image processing of actin filaments in unroofed cells obtained by AFM. J.U. wrote the manuscript with contributions from all the authors.

Acknowledgements

We thank Mr Shuichi Ito, Mr Akira Yagi and Mr Nobuaki Sakai (Olympus Co) for kindly lending the use of the atomic force microscope. The authors also thank Mr Yoichi Ose and Mr Junzo Azuma (Hitachi High-Tech Co) for their cooperation in making the assistance device for sonication unroofing.

Conflict of interests

The authors declare no conflicts of interest.

Funding

Development of Advanced Measurement and Analysis Systems (AMED-SENTAN) programme funded by Japan Agency for Medical Research and Development (AMED) [#18hm0102003s0107 to J.U.]; Grant-in-Aid for Scientific Research [#20K06586 to J.U., #19K06583 to E.U.] from Japan Society of Promotion Science (JSPS).

References

1. Usukura J, Yoshimura A, Minakata S, Youn D, Ahn J, and Cho S J (2012) Use of the unroofing technique for atomic force microscopic imaging of the intra-cellular cytoskeleton under aqueous conditions. *J. Electron. Microsc* 61: 321–326.
2. Usukura E, Narita A, Yagi A, Ito S, and Usukura J An unroofing method to observe the cytoskeleton directly at molecular resolution using atomic force microscopy. *Sci. Rep* 6: 27472.
3. Mazia D, Schatten G, and Sale W (1975) Adhesion of cells to surfaces coated with polylysine. Applications to electron microscopy. *J. Cell Biol* 66: 198 200
4. Vacquier V D (1975) The isolation of intact cortical granules from sea urchin eggs: calcium ions trigger granule discharge. *Dev. Biol* 43: 62–74.
5. Clarke M, Schatten G, Mazia D, and Spudich J A (1975) Visualization of actin fibers associated with the cell membrane in amoebae of *Dictyostelium discoideum*. *Proc. Natl. Acad. Sci. USA* 72: 1758–1762.
6. Heuser J (2000) The production of 'cell cortices' for light and electron microscopy. *Traffic* 1: 545–552.

7. Yumura S, and Kitanishi-Yumura T (1992) Release of myosin II from the membrane-cytoskeleton of *Dictyostelium discoideum* mediated by heavy-chain phosphorylation at the foci within the cortical actin network. *J. Cell Biol* 117: 1231–1239.
8. Nermut M V (1982) The 'cell monolayer technique' in membrane research. *Eur. J. Cell Biol* 28: 160–172.
9. Nermut M V, Williams L D, Stamatoglou S C, and Bissell D M (1986) Ultrastructure of ventral membranes of rat hepatocytes spread on type IV collagen. *Eur. J. Cell Biol* 42: 34–55.
10. Heuser J E, and Kirschner M W (1980) Filament organization revealed in platinum replicas of freeze-dried cytoskeleton. *J. Cell Biol* 86: 212–234.
11. Svitkina T (2007) Electron microscopic analysis of the leading edge in migrating cells. *Methods Cell Biol.* 79: 295–319.
12. Chia J X, Efimova N, and Svitkina T M (2016) Neurite outgrowth is driven by actin polymerization even in the presence of actin polymerization inhibitors. *Mol. Biol. Cell* 27: 3695–3704.
13. Svitkina T (2016) Imaging cytoskeleton components by electron microscopy. *Methods Mol. Biol* 1365: 99–118.
14. Efimova N, and Svitkina T M (2018) Branched actin networks push against each other at adherence junctions to maintain cell-cell adhesion. *J. Cell Biol* 217: 1827–1845.
15. Chikina A S, Svitkina T M, and Alexandrova A Y (2019) Time-resolved ultrastructure of the cortical actin cytoskeleton in dynamic membrane blebs. *J. Cell Biol* 218: 445–454.
16. Yang C, and Svitkina T M (2019) Ultrastructure and dynamics of the actin-myosin II cytoskeleton during mitochondrial fission. *Nat. Cell Biol* 21: 603–613.
17. Kumar A, Shutova M S, Tanaka K, Iwamoto D V, Calderwood D A, Svitkina T M, and Schwartz M A (2019) Filamin a mediates isotropic distribution of applied force across the actin network. *J. Cell Biol* 218: 2481–2491.
18. Heuser J E, and Anderson R G (1989) Hypertonic media inhibit receptor-mediated endocytosis by blocking clathrin-coated pit formation. *J. Cell Biol* 108: 389–400.
19. Heuser J (1989) Effects of cytoplasmic acidification on clathrin lattice morphology. *J. Cell Biol* 108: 401–411.
20. Fujimoto L M, Roth R, Heuser J E, and Schmid S L (2000) Actin assembly plays a variable, but not obligatory role in receptor-mediated endocytosis in mammalian cells. *Traffic* 1: 161–171.
21. Heuser J (2014) Some personal and historical notes on the utility of "deep-etch" electron microscopy for making cell structure/function correlations. *Mol. Biol. Cell* 25: 3273–3276.
22. Engqvist-Goldstein A E Y, Warren R A, Kessels M M, Keen J H, Heuser J, and Drubin D G (2001) The actin-binding protein Hip1R associates with clathrin during early stages of endocytosis and promotes clathrin assembly in vitro. *J. Cell Biol* 154: 1209–1223.
23. Lang T (2003) Imaging SNAREs at work in 'unroofed' cells–approaches that may be of general interest for functional studies on membrane proteins. *Biochem. Soc. Trans* 31: 861–864.
24. Hayakawa E H, Tokumasu F, Usukura J, Matsuoka H, Tsuboi T, and Wellems T E (2015) Imaging of the subsurface structures of "unroofed" plasmodium falciparum-infected erythrocytes. *Exp. Parasitol* 153: 174–179.
25. Sochack K A, and Taraska J W (2017) Correlative fluorescence super-resolution localization microscopy and platinum replica EM on unroofed cells. *Methods Mol. Biol* 1663: 219–230.
26. Aggeler J, and Werb Z (1982) Initial events during phagocytosis by macrophages viewed from outside and inside the cell: Membrane-particle interactions and clathrin. *J. Cell Biol* 94: 613–623.
27. Hartwig J H, Chambers K, and Stossel T P (1989) Association of gelsolin with actin filaments and cell membranes of macrophages and platelets. *J. Cell Biol* 108: 467–479.
28. Fujimoto T, Lee K, Miwa S, and Ogawa K (1991) Immunocytochemical localization of fodrin and ankyrin in bovine chromaffin cells in vitro. *J. Histochem. Cytochem* 39: 1485–1493.
29. Wientjes F, Segal A W, and Hartwig J H (1997) Immunoelectron microscopy shows a clustered distribution of NADPH oxidase components in the human neutrophil plasma membrane. *J. Leukoc. Biol* 61: 303–312.
30. Tzima E, Trotter P J, Orchard M A, and Walker J H (1999) Annexin V binds to the actin-based cytoskeleton at the plasma membrane of activated platelets. *Exp. Cell Res* 251: 185–193.
31. Morone N, Fujiwara T, Murase K, Kasai S, Ike H, Yuasa S, Usukura J, and Kusumi A (2006) Three-dimensional reconstruction of the membrane skeleton at the plasma membrane interface by electron tomography. *J. Cell Biol* 174: 851–862.
32. Morone N (2010) Freeze-etch electron tomography for the plasma membrane interface. *Methods Mol. Biol* 657: 275–286.
33. Sato F, Asakawa H, Fukuma T, and Terada S (2016) Semi-in situ atomic force microscopy imaging of intracellular neurofilaments under physiological conditions through the 'sandwich' method. *Microscopy* 65: 316–324.
34. Makihara M, Watanabe T, Usukura E, Kaibuchi K, Narita A, Tanaka N, and Usukura J (2016) A new approach for the direct visualization of the membrane cytoskeleton in cryo-electron microscopy: a comparative study with freeze-etching electron microscopy. *Microscopy* 65: 488–498.
35. Usukura E, Narita A, Yagi A, Sakai N, Uekusa Y, Imaoka Y, Ito S, and Usukura J (2017) A Cryosectioning technique for the observation of ontracellular otructures and immunocytochemistry of tissues in atomic force microscopy (AFM). *Sci. Rep* 7: 6462.
36. Takahashi M (2005) ξ potential of microbubbles in aqueous solutions: electrical properties of the gas-water interface. *J. Phys. Chem. B* 109: 21858–21864.